Timing observations of three Galactic millisecond pulsars

D.R. Lorimer,[1,2]⋆ A.M. Kawash,[3] P.C.C. Freire,[4] D.A. Smith,[5,6] M. Kerr,[7] M.A. McLaughlin,[1,2] M.B. Mickaliger,[8] R. Spiewak,[8] M. Bailes,[9,10] E. Barr,[4] M. Burgay,[11] A.D. Cameron,[9,10] F. Camilo,[12] S. Johnston,[13] F. Jankowski,[8] E.F. Keane[14], M. Keith,[8] M. Kramer[7] and A. Possenti[9]

[1]*Department of Physics and Astronomy, West Virginia University, Morgantown, WV 26506-6315, USA*
[2]*Center for Gravitational Waves and Cosmology, Chestnut Ridge Building, Morgantown, WV 26505, USA*
[3]*Center for Data Intensive and Time Domain Astronomy, Department of Physics and Astronomy, Michigan State University, East Lansing, MI 48824, USA*
[4]*Max-Planck-Institut für Radioastronomie (MPIfR), Auf dem Hügel 69, D-53121 Bonn, Germany*
[5]*Centre d'Études Nucléaires de Bordeaux Gradignan, IN2P3/CNRS, Université Bordeaux, 33175 Gradignan, France*
[6]*Laboratoire d'Astrophysique de Bordeaux, Université Bordeaux, B18N, allée Geoffroy Saint-Hilaire, 33615 Pessac, France*
[7]*Space Science Division, Naval Research Laboratory, Washington, DC 20375, USA*
[8]*Jodrell Bank Centre for Astrophysics, University of Manchester, Oxford Road, Manchester M13 9PL, UK*
[9]*Centre for Astrophysics and Supercomputing, Swinburne University of Technology, PO Box 218, Hawthorn, VIC 3122, Australia*
[10]*ARC Centre of Excellence for Gravitational Wave Discovery (Ozgrav)*
[11]*INAF, Osservatorio Astronomico di Cagliari, Via della Scienza 5, I-09047, Selargius (CA), Italy*
[12]*South African Radio Astronomy Observatory, Cape Town, South Africa*
[13]*CSIRO Astronomy and Space Science, Australia Telescope National Facility, PO Box 76, Epping NSW 1710, Australia*
[14]*National University of Ireland Galway, University Road, Galway, Ireland H91 TK33*

Accepted 2021 August 27. Received 2021 August 25; in original form 2021 August 09

ABSTRACT

We report observed and derived timing parameters for three millisecond pulsars (MSPs) from observations collected with the Parkes 64-m telescope, Murriyang. The pulsars were found during re-processing of archival survey data by Mickaliger et al. One of the new pulsars (PSR J1546–5925) has a spin period $P = 7.8$ ms and is isolated. The other two (PSR J0921–5202 with $P = 9.7$ ms and PSR J1146–6610 with $P = 3.7$ ms) are in binary systems around low-mass ($> 0.2 M_\odot$) companions. Their respective orbital periods are 38.2 d and 62.8 d. While PSR J0921–5202 has a low orbital eccentricity $e = 1.3 \times 10^{-5}$, in keeping with many other Galactic MSPs, PSR J1146–6610 has a significantly larger eccentricity, $e = 7.4 \times 10^{-3}$. This makes it a likely member of a group of eccentric MSP–He white dwarf binary systems in the Galactic disk whose formation is poorly understood. Two of the pulsars are co-located with previously unidentified point sources discovered with the *Fermi* satellite's Large Area Telescope, but no γ-ray pulsations have been detected, likely due to their low spin-down powers. We also show that, particularly in terms of orbital diversity, the current sample of MSPs is far from complete and is subject to a number of selection biases.

Key words: stars: neutron – pulsars: individual (PSR J0921–5202; PSR J1146–6610; PSR J1546–5925)

1 INTRODUCTION

Understanding the demographics, origin and evolution of pulsars depends strongly on having a well-determined sample based on sensitive surveys. The Parkes radio telescope, also known as Murriyang[1] in Wiradjuri, has been at the forefront of much of this effort. Since the initiation of the Parkes Multibeam Pulsar Survey (Manchester et al. 2001), this and follow-up efforts using the original analogue data acquisition system led to the discovery of 944 pulsars along the Galactic plane and at intermediate and high latitudes (Manchester et al. 2001; Morris et al. 2002; Kramer et al. 2003; Hobbs et al. 2004; Faulkner et al. 2004; Lorimer et al. 2006, 2015; Keith et al. 2009; Eatough et al. 2010; Mickaliger et al. 2012; Eatough et al. 2013; Knispel et al. 2013). Statistical analyses of the sample of pulsars from this and other Parkes Multibeam surveys covering parts of the Southern sky have substantially improved our knowledge of the radio pulsar population (see, e.g, Faucher-Giguère & Kaspi 2006; Lorimer et al. 2006).

Thanks to the Parkes Multibeam surveys and many others over the past two decades (see, e.g., Keith et al. 2010a; Cromartie et al. 2016), the pace of millisecond pulsar (MSP) discoveries has greatly increased. The current sample of MSPs in the Galactic field, which we here define somewhat arbitrarily as pulsars having periods $P <$ 30 ms, now exceeds 400. Of these, 30% were discovered in deep radio searches (Ray et al. 2012) of *Fermi* Large Area Telescope (LAT) γ-ray sources without known counterparts (as in e.g. Abdollahi et al.

⋆ E-mail: duncan.lorimer@mail.wvu.edu (DRL)

[1] The name Murriyang represents the "Skyworld" where a prominent creator spirit of the Wiradjuri Dreaming, Biyaami, lives.

Table 1. Observed and derived parameters of the three MSPs. Timing parameters are specified in Dynamic Barycentric Time (TDB). The orbital parameters were obtained with the ELL1 model (see text for details). Figures in parentheses give the 1-σ uncertainties in the least significant digits. The first distance is estimated from the DM using the (Cordes & Lazio 2002) electron density model, and the second uses the (Yao et al. 2017) electron model. Pseudoluminosities are given as the flux density times distance squared. The minimum companion mass M_c is deduced from the mass function $f = (M_c \sin i)^3/(M_p + M_c)^2$ assuming a pulsar mass $M_p = 1.4\,M_\odot$ and an orbital inclination angle $i = 90$ degrees. Limits on the total proper motion were derived from an independent fit.

Pulsar	PSR J0921–5202	PSR J1146–6610	PSR J1546–5925
General parameters			
Reference epoch (MJD)	57041	57085	57071
Data span (MJD)	56767–57314	56767–59183	56767–57374
Fit χ^2 / number of degrees of freedom	11.98/12	155.66/156	24.76/25
EFAC	1.16	1.26	0.96
Post-fit RMS of residuals (μs)	28.8	53.4	19.8
Right ascension, α (epoch J2000; hh:mm:ss.s)	09:21:59.8785(7)	11:46:58.3731(7)	15:46:29.3456(5)
Declination, δ (epoch J2000; dd:mm:ss.s)	−52:02:38.47(1)	−66:10:51.358(3)	−59:25:44.871(3)
Total proper motion, (mas yr^{-1})	< 216	< 8	< 32
Spin period, P (ms)	9.679813614785(8)	3.722312502674(2)	7.796728856036(2)
First derivative of spin period, $\dot{P}$ (10^{-20} s s^{-1})	1.7(1)	0.793(6)	1.61(3)
Dispersion measure, DM (cm^{-3} pc)	122.4(6)	133.82(1)	168.5(5)
Flux density at 1.4 GHz (mJy)	0.29(2)	0.55(4)	0.67(5)
Orbital parameters			
Orbital period, P_b (d)	38.223675(1)	62.7711887(6)	-
Projected semi-major axis, x (lt sec)	19.05341(2)	22.858617(7)	-
First Laplace-Lagrange parameter, ϵ_1	−0.0000102(14)	0.0071059(7)	-
Second Laplace-Lagrange parameter, ϵ_2	0.0000096(17)	−0.0020616(6)	-
Time of ascending node, $T_{\rm asc}$ (MJD)	56769.836729(6)	56750.930167(8)	-
Derived parameters			
Galactic longitude, l (degrees)	273.78	296.48	323.58
Galactic latitude, b (degrees)	–1.45	–4.12	–3.77
Distance (NE2001, YMW17) (kpc)	1.7, 0.4	2.8, 1.8	3.4, 3.9
Pseudoluminosity at 1.4 GHz (mJy kpc^2)	0.8, 0.04	4.3, 1.8	7.7, 10.2
Spin-down luminosity (10^{25} W)	7.3	61	13
Characteristic age (Gy)	9.1	7.4	7.7
Surface magnetic field strength (10^4 T)	4.1	1.7	3.6
Orbital eccentricity, e	0.0000140(16)	0.0073989(7)	-
Longitude of periastron, ω	313(6)	106.179(5)	-
Time of passage through periastron, T_0	56803.1(7)	56769.4440(9)	-
Mass function, f ($M_\odot$)	0.005083183(14)	0.003254707(3)	-
Minimum companion mass, $M_{\rm c}$ ($M_\odot$)	0.24	0.20	-

2020, hereafter 4FGL). This has led to an era in which some of the new discoveries are known to a relatively small subset of the community prior to publication and their subsequent appearance in the pulsar catalog[2] (Manchester et al. 2005). Since 2012, to broaden the availability of this information prior to full publication, we have maintained an online[3] list of MSPs in the Galactic disk. For each MSP, we list its name, Galactic coordinates, pulse period, dispersion measure and information on the survey(s) which detected it, as well as year of discovery. For binaries, we list preliminary measurements of the orbital period and semi-major axis. In addition, FAST (see e.g. Pan et al. 2021) and MeerKAT (see e.g. Ridolfi et al. 2021) are currently leading a surge in discoveries of MSPs in globular clusters[4].

In this paper, we describe timing observations for three MSPs found during the reprocessing of the Parkes Multibeam Pulsar Survey by Mickaliger et al. (2012), named PSRs J0922−52, J1147−66, and J1546−59 in that work. Timing solutions have already been published for the two other MSPs from that search, PSR J1227−6208 (Bates et al. 2015) and PSR J1725−3853 (Mickaliger et al. 2012). One further MSP found in this analysis, PSR J1753–2822 (Mickaliger 2013), was subsequently timed and described by Perera et al. (2019). In § 2, we describe the observations and present the new timing solutions. In § 3, we discuss specific aspects of these new pulsars and place them in context with what is known about the MSP sample. We present our conclusions and suggestions for future work in § 4.

2 OBSERVATIONS

2.1 Radio timing at Parkes

Regular observations of the three MSPs have been carried out with the central beam of the Parkes Multibeam receiver as part of an organised follow-up campaign that involves participants from a number of different search projects. We used the BPSR back-end (Keith et al. 2010b; Sarkissian et al. 2011) to channelise and record the data as 1024 channels over a 400 MHz band sampled with 8-bit precision and

[2] `https://www.atnf.csiro.au/research/pulsar/psrcat`

[3] `http://astro.phys.wvu.edu/GalacticMSPs`, maintained by Elizabeth C. Ferrara.

[4] `http://www.naic.edu/~pfreire/GCpsr.html`

recorded to disk as 2-bit integers every 64 μs, along with some preliminary observations using the now defunct 1-bit analogue filterbank system, with 512 channels spanning a 256 MHz band (Manchester et al. 2001) sampled every 80 μs.

The latter data were used to compile measurements of barycentric spin periods as a function of time from which we were able to determine preliminary ephemerides (as described, e.g., in Lorimer & Kramer 2004) for all three pulsars, including orbital parameters for the two binary systems, PSR J0921–5202 and PSR J1146–6610. These were then used to fold the BPSR observations to produce `psrfits` formatted pulse profiles (Hotan et al. 2004). All these data were collected between April 2014 and March 2017. For PSR J1146–6610, we made 3 additional observations in October and November 2020, using the UWL receiver and the Medusa back-end (Hobbs et al. 2020).

From each profile, a pulse time of arrival (TOA) was computed by Fourier domain fitting with a noise-free template profile of high signal-to-noise ratio (for details, see Taylor 1992). Due to the generally sparse coverage of the observations at Parkes, the initial orbital solutions for PSR J0921–5202 and PSR J1146–6610 found above were insufficient to phase-connect these two pulsars using standard bootstrapping pulsar timing techniques. To address this, we made use of a new technique recently developed and described in detail by Freire & Ridolfi (2018) in which offsets between groups of TOAs are initially used to refine preliminary ephemerides which are then iteratively examined for pulse numbering ambiguities between epochs to yield a full phase-coherent timing solution[5]. The resulting timing residuals are free from systematic trends.

Table 1 summarizes the spin, astrometric, and orbital parameters. These result from an analysis of the TOAs made using the TEMPO timing software[6], where we used the DE440 Solar System ephemeris (Park et al. 2021) and the Bureau International des Poids et Mesures BIPM2019 time scale. The units are quoted in Dynamic Barycentric Time (TDB). As usual in pulsar timing, we have increased the quoted TOA uncertainties by a factor that is listed in the table as EFAC, in order to obtain a reduced χ^2 of the TOA residuals of 1.0; this results in more realistic uncertainty estimates. The latter are 1-σ equivalent uncertainties, they are indicated in parentheses, and apply to the last digit of their corresponding value. The spin period is quoted for the reference epoch. To minimize correlations between parameters, this epoch is chosen to be near the centre of each data span. The exception is PSR J1146–6610, where it denotes the centre of our earlier data set, without the late 2020 TOAs. The proper motion has not been detected for any of these pulsars; for this reason we derive only upper limits on the total proper motion, which are also presented in Table 1. Hence no corrections to the spindown rate were applied. For a typical transverse MSP velocity of 100 km s^{-1} and the (Cordes & Lazio 2002) dispersion measure (DM) distances in Table 1, the corrected $\dot{P}$ values would be between 67% and 31% of those observed. The expected contributions from Galactic acceleration for these pulsars are much smaller. Using Eqs. 16 and 17 from Lazaridis et al. (2009), we estimate $\dot{P}$ contamination due to this effect to be at the level of (3–9)$\times10^{-22}$.

The orbital parameters for the two binaries (PSR J0921–5202 and PSR J1146–6610) were derived using the ELL1 model (Lange et al. 2001). When the orbital eccentricity, e, is small, the longitude of periastron (ω) is not precisely determined, and it becomes very highly correlated with the time of passage through periastron (T_0);

[5] `https://github.com/pfreire163/Dracula`
[6] `https://sourceforge.net/projects/tempo/`

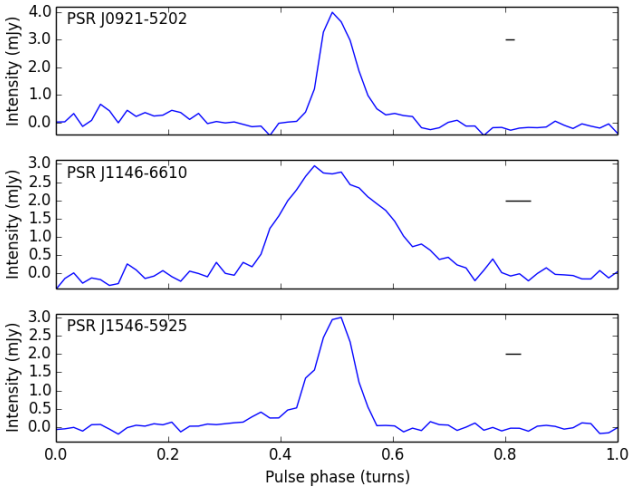

Figure 1. Integrated pulse profiles for the three MSPs. The horizontal lines at phase 0.8 show the effective time resolution of each profile computed from a quadrature sum of the sampling time and dispersion measure smearing (i.e., neglecting the effects of multi-path scattering).

the same happens for P_b and $\dot{\omega}$. The ELL1 model addresses this by referring instead to the time of passage through ascending node, $T_{\rm asc}$, which can be defined precisely even for circular binaries, and using the two Laplace-Lagrange parameters, $\epsilon_1 = e\sin\omega$ and $\epsilon_2 = e\cos\omega$. The downside is that the equations are not exact, but a sum of terms of order xe^n, where x is the projected semi-major axis and n is an integer. The TEMPO and TEMPO2 implementations of this model have recently been updated with terms of order xe^2 (Zhu et al. 2019); this implies that this model can now describe, with great accuracy, most MSP - WD binaries known. This is certainly the case for PSR J0921–5202. For PSR J1146–6610, the magnitude of e implies that the model is borderline applicable: the largest neglected terms, of order xe^3, have a magnitude of 9.3 μs, which is of the same order of magnitude as the error in x, 7.5 μs. Future, more precise timing with MeerKAT (Bailes et al. 2020; Kramer et al. 2021) will require an exact description, like the DD model (Damour & Deruelle 1986), especially if we aim at measuring the Shapiro delay for this system.

In addition to the timing parameters in Table 1, we also provide 1.4-GHz flux density measurements obtained from an analysis of the pulse profiles from each observation. In the absence of a noise diode calibration scheme, for each folded pulse profile, we compute the off-pulse root-mean-square value and then scale the profile so that it matches the expected number in janskys computed from radiometer noise considerations (for details, see Chapter 7 of Lorimer & Kramer 2004). Also taken into account in this calculation is the telescope's offset from the true position of the pulsar found from the timing analysis described above. We assume a Gaussian beam with full-width half maximum of 14′ (Manchester et al. 2001) and scale each profile by the inverse of the degradation factor caused by the offset pointing. As a final step, we integrated the pulse profiles for the three MSPs by summing all the observations, using the timing solutions to achieve phase alignment, as seen in Fig. 1.

2.2 High-energy follow up with the *Fermi* LAT

Given the precise positions for these three MSPs, we have looked for their counterparts at other wavelengths. The presumed helium white dwarf (He WD) companions of PSR J0921–5202 and PSR J1146–6610 can in principle be detected in the optical and near IR bands,

but no sources at the positions of these pulsars were detected in either the DECam plane survey (Schlafly et al. 2018), the deepest optical survey covering the search area, or the 2MASS survey (Skrutskie et al. 2006); and none has a position coincident with any source in the 3rd GAIA data release (Gaia Collaboration et al. 2021). This is not surprising given the large distances and low Galactic latitudes, this means that any companions will likely be significantly reddened by intervening dust.

In what follows, we will elaborate on the search for γ-ray counterparts. Since its launch in 2008, the Large Area Telescope (LAT) on the *Fermi* satellite has detected GeV γ-rays from nearly 300 pulsars, about 250 of which are published at the timing of writing[7]. The first 117 were characterised by Abdo et al. (2013), and the rest will be in the third γ-ray pulsar catalog (in preparation). Half of the pulsars in this sample are MSPs. Steady counterparts for 290 pulsars are in the 4FGL catalog (Data Release 3). Most known γ-ray MSPs are within 4 kpc of Earth and have spin-down power $10^{26} < \dot{E} < 10^{28}$ W. The fraction of known MSPs detected in γ-rays rises from $< 40\%$ to $> 75\%$ over this $\dot{E}$ range (Laffon et al. 2015).

While all three MSPs presented here have distances like currently known γ-ray MSPs, $\dot{E}$ values for PSR J0921–5202 and PSR J1546–5925 lie at the low end of the typical range. PSR J0921–5202 is within the large (0.5°) error ellipse of the faint (5.8σ) source 4FGL J0924.1−5202, while PSR J1546–5925 has no putative counterpart. PSR J1146–6610 has a typical γ-ray MSP $\dot{E}$ and distance, and lies at the edge of the error ellipse for 4FGL J1147.7−6618 (6.5σ steady point source detection). If the two LAT sources correspond to the two pulsars, the γ-ray efficiency $\epsilon = L_\gamma/\dot{E}$ would be near 20% for both, with L_γ the luminosity above 100 MeV for the Yao et al. (2017) DM distances. The γ-ray MSP population covers all latitudes, but these three MSPs have Galactic latitude $-4.1° < b < -1.4°$, where source confusion is high. LAT sensitivity at the pulsar positions, as well as the measured integral energy flux of the two co-located sources, is in the range $3–9 \times 10^{-15}$ W m^{-2}.

We first searched for γ-ray pulsations from the three MSPs following the method of Smith et al. (2019). We selected γ-ray events with energy above 100 MeV within 2° of the timing position. For each event, we calculated the rotational phase corresponding to the photon arrival time using the ephemerides presented in this paper and the *fermi* plugin to Tempo2 (Hobbs et al. 2006). We weighted the photons using the simple prescription in Smith et al. (2019), which involves calculating the probability that a γ-ray of that energy coming from the pulsar could have its angular distance from the pulsar position, given the LAT's energy-dependent angular resolution. For PSR J0921–5202 and PSR J1546–5925, the statistical significance of a deviation from a uniform distribution in the resulting phase histograms was $< 1\sigma$, that is, no evidence for pulsations, both over the ~ 1.5-year ephemeris validity period and over the 12-year LAT data sample. The spectral energy distributions of both co-located sources show significant pulsar-like curvature.

Given its spin-down power and co-location with a 4FGL source, PSR J1146–6610 is the best candidate among the three MSPs for γ-ray counterpart. We searched for γ-ray pulsations using the more sensitive method of Bruel (2019). For this, we descended to 50 MeV and extended to 5°. For both weighting methods, the significance of a putative deviation from a uniform phase distribution was 2.1σ for the full data set, and 2.4σ during the 6.6 yr of ephemeris validity. Smith et al. (2019) showed that in such analyses 4σ significances are required to avoid false positive detections. If the deviation is due to a weak pulsed signal, continued radio timing would provide the phase-connected ephemeris necessary to phase-fold the gamma rays, and a 4σ pulsed gamma-ray detection could appear around 2025.

[7] https://confluence.slac.stanford.edu/display/GLAMCOG/Public+List+of+LAT-Detected+Gamma-Ray+Pulsars

3 DISCUSSION

3.1 Two binary MSPs

Assuming pulsar masses $M_p = 1.4\,M_\odot$, the two new binary MSPs presented in this work, PSR J0921–5202 and PSR J1146–6610, have minimum companion masses $M_c > 0.24$ and $> 0.20\,M_\odot$. For their orbital periods, Tauris & Savonije (1999) predict He WD masses of ~ 0.30 and $\sim 0.32\,M_\odot$, thus compatible with the minimum values of both binaries. If true, the latter values imply that both systems are seen at relatively small orbital inclinations: for the assumed pulsar mass these are about 54° and 41°, respectively. The pulsars themselves are fast-spinning and have very small magnetic fields (see Table 1), in agreement with what is commonly observed among MSP–He WD systems with these orbital periods. The orbital eccentricity of the PSR J0921–5202 system is also in rough agreement with the predictions of Phinney (1992) for its orbital period. However, this is not the case for the PSR J1146–6610 system, where e is about two orders of magnitude larger than that prediction. We discuss this in more detail below.

3.2 Eccentric binary MSPs in the Galactic disk

One of the key predictions of binary stellar evolution theory is that, after recycling of a neutron star via accretion of matter from a stellar companion, the orbit will be circularised by tidal interactions (e.g., Alpar et al. 1982). The system can become eccentric again if the companion undergoes a supernova (e.g., Tauris et al. 2017), but if it evolves instead into a WD, then the orbit should retain a very low eccentricity (Phinney 1992). This is indeed what is observed for the vast majority of recycled pulsars outside globular clusters. In globular clusters, MSPs with high eccentricities arise due to the large stellar densities which can significantly perturb the orbits of pulsar–WD binaries after the recycling (Phinney 1992 and references therein); they can even cause exchanges of companions (e.g., Prince et al. 1991).

However, there are exceptions, which are listed in Table 2. In 2008, a highly eccentric binary MSP, PSR J1903+0327, was discovered in the Galactic disk (Champion et al. 2008). This did not originate in a globular cluster or the Galactic centre, and has a 1 $M_\odot$ main sequence star as a companion (Freire et al. 2011). The most likely hypothesis is that this system formed via the chaotic disruption of a hierarchical triple system (Freire et al. 2011; Portegies Zwart et al. 2011).

Following this, an additional five moderately eccentric ($0.027 < e < 0.14$) MSP binaries have been previously characterized, these are the first five systems in Table 2. They have very similar orbital characteristics. Apart from their eccentricities, their orbital periods are all between 22 and 32 d, occupying a previously identified gap in distribution of orbital periods for binary MSPs. The measured companion masses (see Table 2) are also compatible with the predictions of Tauris & Savonije (1999) for He WDs (for PSR J2234+0611 the companion was confirmed to be a He WD by optical observations, see Antoniadis et al. 2016), although for PSR J1946+3417, the companion mass is somewhat smaller than that expectation.

For PSR J1146–6610, e is two orders of magnitude larger than predicted for its orbital period by Phinney (1992). For this reason we

Table 2. Parameters for the eccentric binary MSPs known in the Galactic disk, ordered by increasing orbital period. This selection excludes the currently known double neutron star binary systems. Note how PSR J1903+0327, which has a confirmed main-sequence star companion, differs from the remaining systems, for which the companions are thought to be He WDs; this has been confirmed for the companion of PSR J2234+0611 (Antoniadis et al. 2016). Although PSR J1146–6610 belongs to the eccentric MSP–He WD systems, it has a few important differences from the others. For PSR J1903+0327, the uncertainties on the masses are strongly non-Gaussian, they are presented here to 99.7% confidence limit. For systems where there are no published masses yet, we calculate a minimum companion mass assuming the pulsar mass in square brackets.

PSR	P (ms)	P_b (d)	e	M_p ($M_\odot$)	M_c ($M_\odot$)	References
J1950+2414	4.3048	22.1914	0.0798	1.496(23)	$0.280^{+0.005}_{-0.005}$	Knispel et al. (2015); Zhu et al. (2019)
J1618−3921	11.9873	22.7456	0.0274	[1.4]	> 0.18	Edwards & Bailes (2001); Octau et al. (2018)
J0955−6150	1.9993	24.5784	0.1175	[1.4]	> 0.22	Camilo et al. (2015)
J1946+3417	3.1701	27.0199	0.1345	1.828(22)	0.2556(19)	Barr et al. (2013, 2017)
J2234+0611	3.5766	32.0014	0.1293	$1.353^{+0.014}_{-0.017}$	$0.298^{+0.015}_{-0.012}$	Deneva et al. (2013); Stovall et al. (2019)
J1146–6610	3.7223	62.7712	0.0074	[1.4]	> 0.20	This paper
J1903+0327	2.1499	95.1741	0.4367	1.667(21)	1.029(8)	Champion et al. (2008); Freire et al. (2011)

consider it the seventh eccentric MSP system known in the Galactic disk. Its companion mass is consistent with that of a He WD, however, its orbital period is $\gtrsim 2$ times larger and e is one order of magnitude smaller than those of the other eccentric MSP–He WD systems, a combination of characteristics that makes PSR J1146–6610 unique. In what follows, we will discuss the formation of these enigmatic systems.

3.3 Formation of eccentric MSPs

The orbital similarities of the first five systems in Table 2 suggest that their origin is a well-defined stellar evolution mechanism with a predictable outcome, unlike the chaotic disruption of a triple system that is thought to have formed PSR J1903+0327. Two hypothetical mechanisms (Freire & Tauris 2014; Jiang et al. 2015) suggest that these eccentricities result from the release of gravitational binding energy that happens in a phase transition in the object that later becomes the MSP. This necessarily occurs after the mass transfer phase has ended, otherwise the system would re-circularize. This delayed collapse is therefore not caused by mass accretion, it is caused instead, in both hypotheses, by the spin-down of the progenitor to the MSP, which slowly decreases the centrifugal force, and thus leads to a steady increase in the central pressure.

As discussed by Tauris et al. (2017), if a circular binary loses an amount of mass ΔM in an amount of time that is small compared to the orbital period, and there is no kick involved – i.e., a symmetric SN – the post-SN eccentricity

$$e = \frac{\Delta M}{M_T}, \tag{1}$$

where M_T is the total mass of the binary after the mass loss. Given the binding energies of neutron stars, the expected post-SN eccentricities are of the order of 0.1, as observed for the first five eccentric binary MSPs in Table 2.

Although these hypotheses naturally predict not only the observed eccentricities, but also the observed orbital periods, they also predict a rather narrow set of masses for the resulting MSPs, e.g. Freire & Tauris (2014) predict $1.22 M_\odot < M_p < 1.27 M_\odot$. Jiang et al. (2015) predict larger masses, depending on the unknown threshold for the central density at which the hypothetical phase transition occurs. Using models with fast rotating neutron stars, they predict a range from 1.4 to $> 2\,M_\odot$. Such focused MSP masses are incompatible with the mass measurements in Table 2, which span a wide range from 1.35 to $1.83 M_\odot$.

Furthermore, such a phase transition is not a likely formation mechanism for PSR J1146–6610: as mentioned above, the expected eccentricities are too large. The simulations made by Freire & Tauris (2014) suggest that, for any scenario involving a phase transition, fine tuning of mass loss and kick direction and magnitude would be necessary to obtain $e \sim 0.0074$.

An alternative hypothesis, put forward by Antoniadis (2014), postulates that the eccentricities of these systems arise from the dynamical interaction of the binary with a circumbinary disk, which results from thermonuclear hydrogen flashes at the surface of the WD. This hypothesis is compatible with the wide range of MSP masses measured for these systems, and it predicts that the eccentric MSP–WD systems have a relatively wide range of orbital periods, from well below 10 d to a maximum of ~ 50 d. The latter value corresponds, according to the relation of Tauris & Savonije (1999), to the critical He WD mass above which hydrogen flashes cease, then thought to be $\sim 0.31\,M_\odot$. More recently, Han & Li (2021) have suggested that these orbital eccentricities might be the result of a collection of small kicks to the companion WD caused by these thermonuclear flashes. They note that there is currently no consensus on the upper WD mass limit for which hydrogen flashes occur, and suggest that the observed range of orbital periods for the eccentric MSPs could be used for determining this number.

Thus, if either hypothesis is correct, the eccentricity and orbital periods of PSR J1146–6610 imply that some amount of thermonuclear activity can still happen for WDs with the mass of the companion of PSR J1146–6610, which, according to the relation of Tauris & Savonije (1999) is $\sim 0.32\,M_\odot$.

Very recently, the work of Phinney (1992) has been expanded by Ginzburg & Chiang (2021) in an attempt to explain the high eccentricities of these pulsars. This hypothesis explains the orbital eccentricities in terms of coherent resonances between the orbital period and the timescale of convective eddys in the red giant progenitors, which had already been estimated by Phinney (1992) to be ∼25 d. To construct a viable model, Ginzburg & Chiang had to assume that in resonance - and only in resonance - the convection stops being random. This explains the characteristics of the eccentric MSPs well, especially their orbital periods: the 25-d periodicity lies near the middle of their range of orbital periods. However, it is not yet clear whether this hypothesis can explain the eccentricity of PSR J1146–6610 which has a much longer orbital period. Perhaps it is in a weaker 1:2 resonance with the convection turnover time. The orbital

period distribution of many more future eccentric MSP discoveries might allow the identification of such multiple resonances.

3.4 The Galactic MSP population

We conclude with some brief remarks concerning the state of MSP statistics and demography. From the earliest days of this field, when the sample numbered only a few objects, much debate has taken place on the birth rate and population size of MSPs both in the Galaxy and its globular cluster systems. The modest addition of these three pulsars to the observed sample is perhaps notable by the fact that discoveries are still being made of objects which buck the trend based on previous understanding. While population analyses can now make use of a sample that is much larger than in previous years and are strongly encouraged, it is important to realize that these "outlier" pulsars such as PSR J1146–6610 still being found indicates that the sample is still heavily biased by observational selection. MSPs discovered using the γ-ray unassociated sources have broadened the selection (Ray et al. 2012), but substantial bias remains.

One way to see the limitations of the observed sample is shown in Fig. 2. In the left panel, we show the observed sample as a scatter diagram in the DM–P plane. Most of the currently known MSPs have DMs in the range 10–100 cm^{-3} pc. The right-hand panel of Fig. 2 shows the results of a simple Monte Carlo simulation and our current model of the underlying MSP population. The Monte Carlo pulsars were generated using the `psrpop` software package (Lorimer et al. 2006) and was normalized to mimic the sample of 60 MSPs given in Lorimer et al. (2015) and adopting the period distribution derived in that study. For the purposes of this demonstration, we adopt a 500 pc scale height, 10% duty cycle for intrinsic pulse widths, and take the underlying luminosity distribution to be log-normal, as found for the normal pulsar population (Lorimer et al. 2006). It is particularly striking that the mean DM value in the population as a whole is much larger than in the observed sample, and that there is a significant number of pulsars with DM/P > 150 cm^{-3} pc ms^{-1} that are yet to be discovered.

4 CONCLUSIONS

We have presented high-precision timing measurements for three Galactic MSPs. One of these is apparently solitary (PSR J1546–5925) while the other two (PSR J0921–5202 and PSR J1146–6610) are in binary systems. The three timing solutions presented in this paper significantly improve upon what was known about each pulsar prior to this work. The pulsars themselves are generally quite weak and close to the detection threshold available with Parkes. For this reason, the TOA precision is relatively poor, making the derivation of their timing solutions unusually difficult. This required the use of the innovative algorithm described by Freire & Ridolfi (2018). In particular, PSR J1146–6610 was perhaps the most challenging pulsar ever phase connected with this algorithm; this required the vast improvement in efficiency provided by the implementation of the partial solution prioritisation described in the last paragraph of section 4.3 of Freire & Ridolfi (2018). Even with this improvement, the algorithm still needed to analyse 173,311 partial solutions before finding the correct rotation count for PSR J1146–6610; this took about 8 hours on a single core.

Our work showed that PSR J1146–6610 has an anomalously high orbital eccentricity when compared to most low-mass binary MSPs and we speculate that it is a member of a group of unusually eccentric MSP–He WD binaries for which the formation mechanism is not yet well understood.

Our current timing precision and data span prevent the measurement of proper motions, parallaxes and post-Keplerian effects such as the rate of advance of periastron ($\dot{\omega}$) or the Shapiro delay. Some of these effects will be measurable with MeerKAT (Bailes et al. 2020) observations: PSR J0921–5202 and PSR J1546–5925 were observed by Spiewak et al. (in prep) and seen with S/N > 50 in < 30 minutes. The dense MeerKAT timing campaigns carried out by the relativistic binaries program (Kramer et al. 2021) will be able to measure the $\dot{\omega}$ of PSR J1146–6610 to high significance, and thus determine its total mass, although this will likely need a couple of orbital campaigns spaced by a few years. If the low orbital inclinations inferred above for PSR J0921–5202 and PSR J1146–6610 are correct, then a detection of the Shapiro delay will be difficult for either system, even with dense MeerKAT campaigns, and will likely have to wait for instruments like the Square Kilometre Array. Long-term, low-cadence observations will measure the proper motions and increase the sensitivity to γ-ray pulsations for the three pulsars. Such measurements could reveal additional companions to these pulsars that are not currently detectable (e.g., as for PSR J1024−0719, Kaplan et al. 2016; Bassa et al. 2016).

Finally, we highlight that the MSP sample is incomplete and predict that further unusual discoveries will be made as we better sample the Galactic MSP zoo. Currently, these rare moderately eccentric MSPs allow a glimpse into the final evolution of mass transfer/mass loss in binary pulsars. As we discover more, the bulk properties of the population will enable us to determine at what orbital separations and donor masses episodic mass loss may be important.

DATA AVAILABILITY

The data underlying this article will be shared on reasonable request to the corresponding author.

ACKNOWLEDGEMENTS

We thank Paul Ray, Ben Perera and the anonymous referee for useful comments on an earlier version of this manuscript. DRL and MAM acknowledge support from the NSF awards AAG-1616042, OIA-1458952 and PHY-1430284.

Work at NRL is supported by NASA. We acknowledge the Wiradjuri people as the traditional owners of the Observatory site. The Parkes telescope ("Murriyang") is part of the Australia Telescope National Facility which is funded by the Commonwealth of Australia for operation as a National Facility managed by CSIRO.

The *Fermi* LAT Collaboration acknowledges generous ongoing support from a number of agencies and institutes that have supported both the development and the operation of the LAT as well as scientific data analysis. These include the National Aeronautics and Space Administration and the Department of Energy in the United States, the Commissariat à l'Energie Atomique and the Centre National de la Recherche Scientifique / Institut National de Physique Nucléaire et de Physique des Particules in France, the Agenzia Spaziale Italiana and the Istituto Nazionale di Fisica Nucleare in Italy, the Ministry of Education, Culture, Sports, Science and Technology (MEXT), High Energy Accelerator Research Organization (KEK) and Japan Aerospace Exploration Agency (JAXA) in Japan, and the K. A. Wallenberg Foundation, the Swedish Research Council and the Swedish National Space Board in Sweden.

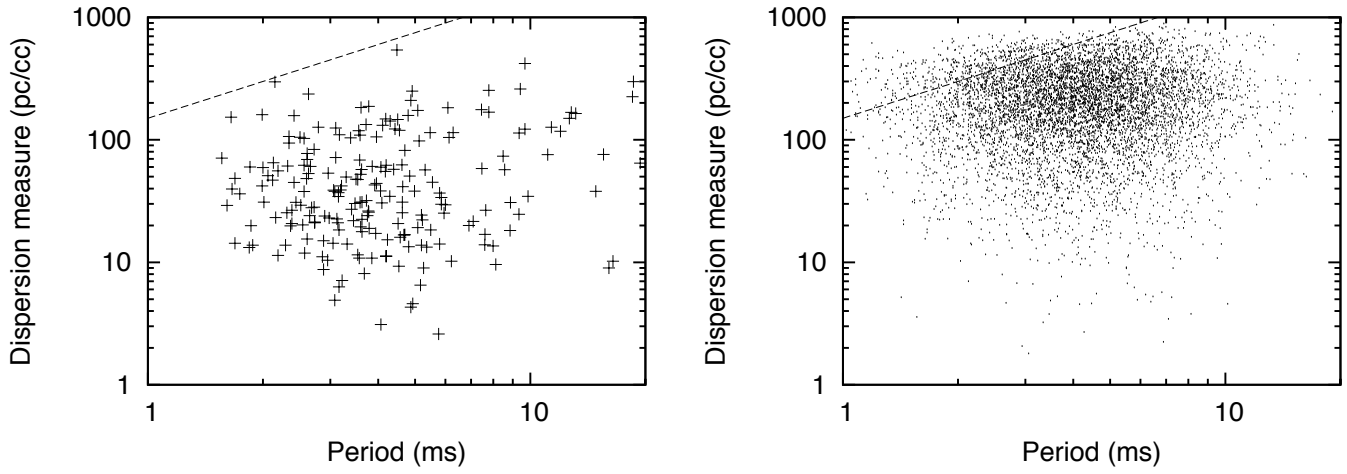

Figure 2. Left: DM versus P for the current sample of MSPs. Right: DM versus P for a fake sample of model pulsars in which no selection effects are applied. The dashed line shown in both plots is the locus of points for which $\mathrm{DM}/P = 150\ \mathrm{cm}^{-3}\ \mathrm{pc\ ms}^{-1}$.

Additional support for science analysis during the operations phase is gratefully acknowledged from the Istituto Nazionale di Astrofisica in Italy and the Centre National d'Études Spatiales in France. This work performed in part under DOE Contract DE-AC02-76SF00515.

REFERENCES

Abdo A. A., et al., 2013, ApJS, 208, 17
Abdollahi S., et al., 2020, ApJS, 247, 33
Alpar M. A., Cheng A. F., Ruderman M. A., Shaham J., 1982, Nature, 300, 728
Antoniadis J., 2014, ApJ, 797, L24
Antoniadis J., Kaplan D. L., Stovall K., Freire P. C. C., Deneva J. S., Koester D., Jenet F., Martinez J. G., 2016, ApJ, 830, 36
Bailes M., et al., 2020, Publ. Astron. Soc. Australia, 37, e028
Barr E. D., et al., 2013, MNRAS, 435, 2234
Barr E. D., Freire P. C. C., Kramer M., Champion D. J., Berezina M., Bassa C. G., Lyne A. G., Stappers B. W., 2017, MNRAS, 465, 1711
Bassa C. G., et al., 2016, MNRAS, 460, 2207
Bates S. D., et al., 2015, MNRAS, 446, 4019
Bruel P., 2019, A&A, 622, A108
Camilo F., et al., 2015, ApJ, 810, 85
Champion D. J., et al., 2008, Science, 320, 1309
Cordes J. M., Lazio T. J. W., 2002, arXiv e-prints, pp astro–ph/0207156
Cromartie H. T., et al., 2016, ApJ, 819, 34
Damour T., Deruelle N., 1986, Ann. Inst. Henri Poincaré Phys. Théor, 44, 263
Deneva J. S., Stovall K., McLaughlin M. A., Bates S. D., Freire P. C. C., Martinez J. G., Jenet F., Bagchi M., 2013, ApJ, 775, 51
Eatough R. P., Molkenthin N., Kramer M., Noutsos A., Keith M. J., Stappers B. W., Lyne A. G., 2010, MNRAS, 407, 2443
Eatough R. P., Kramer M., Lyne A. G., Keith M. J., 2013, MNRAS, 431, 292
Edwards R. T., Bailes M., 2001, ApJ, 553, 801
Faucher-Giguère C.-A., Kaspi V. M., 2006, ApJ, 643, 332
Faulkner A. J., et al., 2004, MNRAS, 355, 147
Freire P. C. C., Ridolfi A., 2018, MNRAS, 476, 4794
Freire P. C. C., Tauris T. M., 2014, MNRAS, 438, L86
Freire P. C. C., et al., 2011, MNRAS, 412, 2763
Gaia Collaboration et al., 2021, A&A, 649, A1
Ginzburg S., Chiang E., 2021, MNRAS
Han Q., Li X.-D., 2021, ApJ, 909, 161
Hobbs G., et al., 2004, MNRAS, 352, 1439
Hobbs G. B., Edwards R. T., Manchester R. N., 2006, MNRAS, 369, 655
Hobbs G., et al., 2020, Publ. Astron. Soc. Australia, 37, e012
Hotan A. W., van Straten W., Manchester R. N., 2004, Publ. Astron. Soc. Australia, 21, 302
Jiang L., Li X.-D., Dey J., Dey M., 2015, ApJ, 807, 41
Kaplan D. L., et al., 2016, ApJ, 826, 86
Keith M. J., Eatough R. P., Lyne A. G., Kramer M., Possenti A., Camilo F., Manchester R. N., 2009, MNRAS, 395, 837
Keith M. J., et al., 2010a, MNRAS, 409, 619
Keith M. J., et al., 2010b, MNRAS, 409, 619
Knispel B., et al., 2013, ApJ, 774, 93
Knispel B., et al., 2015, ApJ, 806, 140
Kramer M., et al., 2003, MNRAS, 342, 1299
Kramer M., et al., 2021, MNRAS, 504, 2094
Laffon H., Smith D. A., Guillemot L., 2015, Proc. 5^{th} *Fermi* Symposium - eConf C141020.1,
Lange C., Camilo F., Wex N., Kramer M., Backer D. C., Lyne A. G., Doroshenko O., 2001, MNRAS, 326, 274
Lazaridis K., et al., 2009, MNRAS, 400, 805
Lorimer D. R., Kramer M., 2004, Handbook of Pulsar Astronomy. Cambridge, UK
Lorimer D. R., et al., 2006, MNRAS, 372, 777
Lorimer D. R., et al., 2015, MNRAS, 450, 2185
Manchester R. N., et al., 2001, MNRAS, 328, 17
Manchester R. N., Hobbs G. B., Teoh A., Hobbs M., 2005, AJ, 129, 1993
Mickaliger M. B., 2013, PhD thesis, West Virginia University
Mickaliger M. B., et al., 2012, ApJ, 759, 127
Morris D. J., et al., 2002, MNRAS, 335, 275
Octau F., Cognard I., Guillemot L., Tauris T. M., Freire P. C. C., Desvignes G., Theureau G., 2018, A&A, 612, A78
Pan Z., et al., 2021, arXiv e-prints, p. arXiv:2106.08559
Park R. S., Folkner W. M., Williams J. G., Boggs D. H., 2021, AJ, 161, 105
Perera B. B. P., et al., 2019, MNRAS, 487, 1025
Phinney E. S., 1992, Philosophical Transactions of the Royal Society of London Series A, 341, 39
Portegies Zwart S., van den Heuvel E. P. J., van Leeuwen J., Nelemans G., 2011, ApJ, 734, 55
Prince T. A., Anderson S. B., Kulkarni S. R., Wolszczan A., 1991, ApJ, 374, L41
Ray P. S., et al., 2012, preprint, (`arXiv:1205.3089`)
Ridolfi A., et al., 2021, MNRAS, 504, 1407
Sarkissian J. M., Carretti E., van Straten W., 2011, in Burgay M., D'Amico N., Esposito P., Pellizzoni A., Possenti A., eds, American Institute of Physics Conference Series Vol. 1357, American Institute of Physics Conference Series. pp 351–352, doi:10.1063/1.3615155

Schlafly E. F., et al., 2018, ApJS, 234, 39
Skrutskie M. F., et al., 2006, AJ, 131, 1163
Smith D. A., et al., 2019, ApJ, 871, 78
Stovall K., et al., 2019, ApJ, 870, 74
Tauris T. M., Savonije G. J., 1999, A&A, 350, 928
Tauris T. M., et al., 2017, ApJ, 846, 170
Taylor J. H., 1992, Philosophical Transactions of the Royal Society of London Series A, 341, 117
Yao J. M., Manchester R. N., Wang N., 2017, ApJ, 835, 29
Zhu W. W., et al., 2019, ApJ, 881, 165

This paper has been typeset from a TEX/LATEX file prepared by the author.